# Amplifiers for bioelectric events: a design with a minimal number of parts

**A. C. MettingVanRijn  A. Peper  C. A. Grimbergen**

Department of Medical Physics & Informatics, University of Amsterdam, Faculty of Medicine, Meibergdreef 15, 1105 AZ Amsterdam, The Netherlands

**Abstract**—*A design for an amplifier for bioelectric events is presented that has fewer parts than conventional designs. The design allows the construction of amplifiers of a high quality in terms of noise and common mode rejection, with reduced dimensions and with a lower power consumption. Gain, bandwidth and number of channels are easily adapted to a wide range of biomedical applications. An application example is given in the form of a multichannel EEG amplifier (gain is 20 000), in which each channel consists of three operational amplifiers (one single and one dual), six resistors and two capacitors. The equivalent input noise voltage and current are 0.15 $\mu V_{rms}$ and 1 $pA_{rms}$, respectively, in a bandwidth of 0.2–40 Hz, and a common mode rejection ratio of 136 dB is achieved without trimming.*

**Keywords**—*Common mode rejection ratio, DC suppression, Instrumentation amplifier, Number of parts, Recording of bioelectric events*

Med. & Biol. Eng. & Comput., 1994, 32, 305–310

## 1 Introduction

THE SPECIFICATIONS required for an amplifier for bioelectric events are high overall gain (1000–100 000), low equivalent input noise density ($<100\ nV/\sqrt{Hz}$ with typical electrode impedances) (COOPER *et al.*, 1969; SILVERMAN *et al.*, 1969), high common mode input impedance ($>100\ M\Omega$ at 50 Hz) (PACELA, 1967) and a high common mode rejection ratio (CMRR) ($>80$ dB at 50 Hz) (HUHTA and WEBSTER, 1973). The design of amplifiers for bioelectric events is complicated by electrode offset voltages; DC input voltages of up to 200 mV should not result in saturation of the amplifier (GEDDES, 1972).

In addition, some features are important to obtain a practical design; no severe demands should be put on resistor matching, nor should additional trimming be necesseay. The importance of a low capacitance between the isolated section of the measurement system, containing the amplifier, and the environment (METTINGVANRIJN *et al.*, 1991*b*) has two implications for the design of the amplifier; power consumption should be low to enable small-sized batteries to be used as a power supply, and the dimensions of the amplifier should be kept to a minimum. A low power consumption can partly be achieved by minimising the number of active parts (transistors, FETs and operational amplifiers). Small dimensions call for a design with a low total number of parts and without capacitors larger than 100 nF or inductors to allow for surface mount or thick-film construction.

## 2 Instrumentation amplifiers

An amplifier for bioelectric events is an instrumentation amplifier; a differential amplifier with fixed differential gain, a high input impedance, a high CMRR and low noise. There are two groups of designs for instrumentation amplifiers; the long-tailed pair with current feedback (GRAEME, 1977), and the designs built with operational amplifiers (op-amps). In principle, the first group offers the best performance, especially when high-quality discrete parts are used (NELSON, 1980), but the realisations tend to be rather complex (METTINGVANRIJN *et al.*, 1991*a*). There are some monolithic versions of long-tailed pair designs (e.g. AMP01 and LM363). However, these ICs lack the flexibility needed in amplifiers for bioelectric events; it is difficult to obtain DC suppression (SMIT *et al.*, 1987) and to adapt the designs for monopolar multichannel recordings (METTINGVANRIJN *et al.*, 1990).

The use of op-amps as active elements is an attractive way to construct a relatively simple instrumentation amplifier. There are two basic designs; the two op-amp (Fig. 1) and the three-op-amp instrumentation amplifier (TOBEY

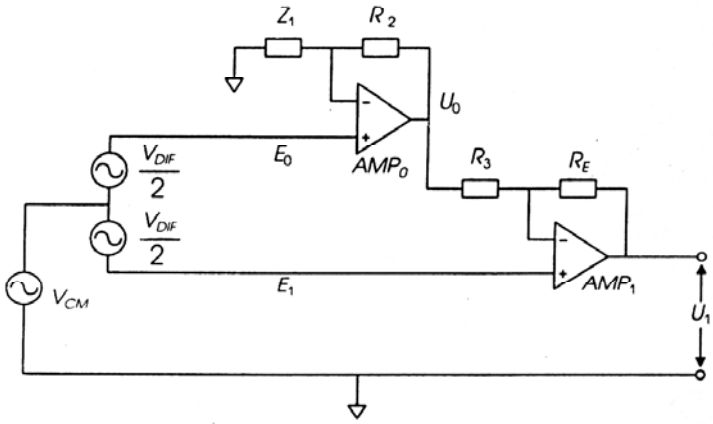


**Fig. 1** *Basic instrumentation amplifier with two operational amplifiers; features of the circuit are a fixed differential voltage gain, a high common mode rejection ratio, high input impedances and low noise*

*First received 14 May 1992 and in final form 15 March 1993*

*et al.*, 1971; HOROWITZ and HILL, 1989). The two-op-amp design has, in principle, some drawbacks in comparison with the three-op-amp design; the common mode input range is lower, and the matching of the resistors is more critical if a high CMRR is to be achieved (GRAEME, 1973). However, these drawbacks become less important at high values of overall gain (as is the case with biomedical measurements), and the important advantage of a simpler design remains.

Neither of the above instrumentation amplifiers can be used without modifications as an amplifier with high gain for the recording of bioelectric events, because the electrode offset voltages would cause saturation of the amplifier. The usual solution is to employ the three-op-amp instrumentation amplifier with moderate gain (approximately 30 dB) in the first amplifier stage, followed by several AC-coupled amplifier stages to achieve a high overall gain combined with a low offset voltage at the amplifier output (NEUMAN, 1978; METTINGVANRIJN *et al.*, 1991*b*).

In this paper, instead of the more widely used three-op-amp instrumentation amplifier, the two-op-amp instrumentation amplifier is used as a basis for an amplifier for bioelectric events. Before modifying the two-op-amp instrumentation amplifier for biomedical applications, some features of the basic circuit are reviewed.

The common mode gain of a two-op-amp instrumentation amplifier becomes zero if the relevant impedances (resistors $R_2$, $R_3$, $R_E$ and impedance $Z_1$ in Fig. 1) are chosen according to

$$\frac{Z_1}{R_2} = \frac{R_E}{R_3} \tag{1}$$

If the condition in eqn. 1 is fulfilled, the differential gain of a two-op-amp instrumentation amplifier is given by

$$A_{DIF} = \left(\frac{R_E}{R_3} + 1\right) \tag{2}$$

In practice, the CMRR of a two-op-amp instrumentation amplifier depends on the matching of the resistors and the chosen differential gain. A good approximation for the CMRR with small deviations from the exact resistor ratios is given by

$$\text{CMRR} = 20\log\left(\frac{100}{2\,TOL_R}\right) + 20\log A_{DIF} \quad (\text{in dB}) \tag{3}$$

where $TOL_R$ is the resistor tolerance in %.

For example, if the usual 1% tolerance resistors are used for an instrumentation amplifier with a gain of 1000, a CMRR of 94 dB is achieved without trimming.

The good CMRR of a two-op-amp instrumentation amplifier with a high differential gain is a result of the gain of common mode signals ($A_{CM}$) being less than unity, even in cases where the resistor values differ by a large amount from the ratios given in eqn. 1. This effect becomes readily apparent when the gain of the instrumentation amplifier with $R_2 = 0$ (resistor ratios maximally unmatched) is considered for both differential and common mode input signals (in this case, $A_{CM} \approx 1$, $A_{DIF}$ is given by eqn. 2, and CMRR = $A_{DIF}$).

The op-amps in a two-op-amp instrumentation amplifier contribute equally to the equivalent input noise. The two-op-amp instrumentation amplifier has good noise properties, because an insignificant contribution from noise sources other than the input op-amps can be achieved with the gain settings and source impedances found in biomedical recordings. Note that the noise properties of the two-op-amp instrumentation amplifier are equal to those of the three-op-amp instrumentation amplifier if the latter has sufficient gain in the first amplifier stage.

## 3 Novel design for an amplifier for bioelectric events

The two-op-amp design seems attractive for the measurement of bioelectric events because the gain bandwidth product (GBP) of many commerically available low-noise op-amps is high enough to provide for sufficient differential gain in the bandwidth required. For example, both EEG (gain 10 000 and a bandwidth of 30 Hz) and ECG (gain 1000 and a bandwidth of 300 Hz) measurements require a GBP of approximately 300 kHz. Consequently, a single-stage amplifier, with one low-noise op-amp providing all the gain, would suffice.

The problem of adapting the two-op-amp instrumentation amplifier to the biomedical measurement situation means providing the amplifier with a proper high-pass response and a sufficient DC input range, without jeopardising qualities such as high CMRR and low noise. We achieved this goal with the novel circuit shown in Fig. 2.

The common mode gain of the modified two-op-amp instrumentation amplifier in Fig. 2 is zero if

$$\frac{Z_1}{R_2} = \frac{R_4R_5 + R_3R_6 + R_4R_6}{R_3R_5} \tag{4}$$

Provided the condition in eqn. 4 is met, the differential gain $A_{DIF}$ in the passband is

$$A_{DIF} = \left(\frac{R_4}{R_3} + 1\right)\left(\frac{R_6}{R_5} + 1\right) \tag{5}$$

Note that eqs. 4 and 5 correspond to eqs. 1 and 2 if the following substitution is made:

$$R_E \rightarrow \frac{R_4R_5 + R_3R_6 + R_4R_6}{R_5} \tag{6}$$

The circuit in Fig. 2 is a two-op-amp instrumentation amplifier with an integrator in the feedback loop ($AMP_2$ in Fig. 2). The integrator provides a low overall gain for low-frequency input signals. The high-pass corner frequency is set with $R_A$ and $C_A$.

The connection between $R_5$, $R_A$ and the output of $AMP_0$ is essential to attain a high CMRR because it limits the gain for common mode input signals $A_{CM}$ to unity (if $R_5$ and $R_A$ were connected to common, the behaviour for differential input signals would be identical, whereas $A_{CM}$ would

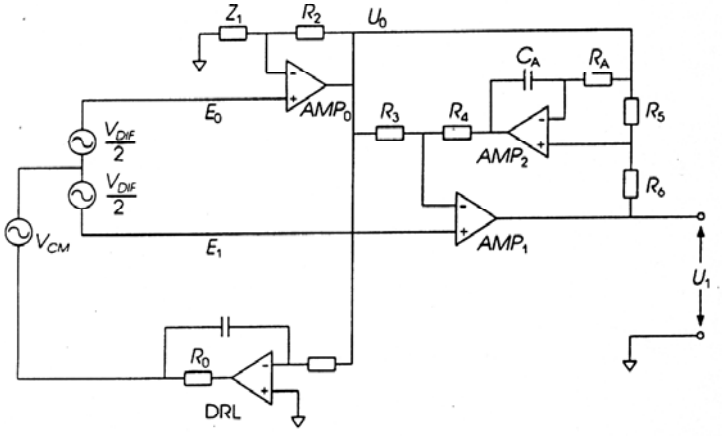


**Fig. 2** *Novel design of an amplifier for bioelectric events based on the two-op-amp instrumentation amplifier; high-pass response is achieved with an integrator in the feedback loop*

become very dependent on exact resistor matching). As a result, eqn. 3 is valid for the modified two-op-amp instrumentation amplifier in Fig. 2, for frequencies above the high-pass cut-off frequency, and the good CMRR properties of the basic two-op-amp instrumentation amplifier are retained.

Below the high-pass cut-off frequency, the common mode gain of the amplifier in Fig. 2 rises by 6 dB per octave to a maximal value of unity. Consequently, for frequencies below the high-pass cut-off frequency, the CMRR drops from the value given by eqn. 3 to a value equal to $A_{DIF}$.

In Fig. 2, a driven right-leg (DRL) circuit is used as a connection between the signal source and the amplifier common (0 V, the midpoint between the supply voltages). A DRL circuit reduces the common mode voltage by driving $U_0$ (Fig. 2) actively to the potential of the amplifier common (METTINGVANRIJN *et al.*, 1990). In addition, a DRL protects the patient from the consequences of amplifier defects, because a series resistor in the circuit ($R_0$ in Fig. 2) limits the maximum current through the ground electrode to a safe level. The common mode suppression of a DRL circuit increases with decreasing frequency. Consequently, the DRL circuit compensates for the decreasing CMRR of the instrumentation amplifier in Fig. 2 at low frequencies.

In our view, a DRL should be used in every biomedical recording system for interference suppression and patient safety. Therefore, when the instrumentation amplifier of Fig. 2 is compared with other designs with respect to the number of parts needed, the DRL circuit should not be regarded as a particular complexity of the design in Fig. 2.

Besides the high CMRR, the good noise properties of the basic two-op-amp instrumentation amplifier are retained as well in the modified two-op-amp instrumentation amplifier in Fig. 2. The extra noise generated by $AMP_2$ is divided by the factor $R_3/(R_3 + R_4)$ (approximately 10–30 in typical biomedical applications; see Section 4) before it is added to the input of $AMP_1$. Consequently, the equivalent input noise level of the circuit is not significantly higher than the combined input noise of op-amps $AMP_0$ and $AMP_1$.

The low-pass corner frequency of the modified two-op-amp instrumentation amplifier depends on the GBP of op-amp $AMP_1$ and the selected differential gain (the op-amps in this Section are assumed to be internally compensated):

$$f_{-3\text{dB}} = \frac{GBP_1}{A_{DIF}} \tag{7}$$

where $GBP_1$ is the gain bandwidth product of op-amp $AMP_1$, and $A_{DIF}$ is the differential gain of the amplifier.

The slope of the amplitude characteristic is $-6$ dB per octave above this frequency. It was established that the differences in GBP between different op-amps of one type were only a few percent for most popular types. Consequently, employing the limited GBP of op-amps was found to be a convenient method of providing the needed low-pass response with sufficient accuracy in the cut-off frequency.

The design is unconditionally stable, and no resonances occur with typical compensated op-amps and the usual gains used in recordings of bioelectric events (see the Appendix).

## 4 Practical considerations

The output voltage of op-amp $AMP_2$ in the circuit shown in Fig. 2 is equal to the DC voltage between the amplifier inputs ($E_0$ and $E_1$) multiplied by the ratio $(R_3 + R_4)/R_3$. However, as the output voltage of op-amp $AMP_2$ is limited by the supply voltage, the DC input range is determined by the resistor ratio $(R_3 + R_4)/R_3$, and a high value for this ratio reduces the maximum allowable electrode offset. On the other hand, a low ratio $(R_3 + R_4)/R_3$ allows noise from $AMP_2$ to contribute significantly to the total amplifier noise. Therefore, a trade-off has to be made between the DC input range and the total noise figure.

The offset voltage at the amplifier output $U_1$ of the circuit in Fig. 2 is the input offset voltage of op-amp $AMP_2$ multiplied by the resistor ratio $(R_5 + R_6)/R_5$. In cases where a high differential gain $A_{DIF}$ is chosen, the output offset can become unacceptably high, even if $AMP_2$ is of a low offset type. A solution is the addition of a second integrator, as shown in Fig. 3 (integrator around $AMP_3$). The output offset of an amplifier channel ($U_1 \ldots U_N$) in Fig. 3 is equal to the input offset of op-amp $AMP_3$.

The op-amps used for the integrators in the circuits shown in Figs. 2 and 3 should have low input bias currents (i.e. JFET, MOSFET or CMOS type op-amps) to allow the selection of large resistances $R_A$ and $R_B$ (which is necessary to reduce the size of the integrator capacitors $C_A$ and $C_B$) without producing large offset voltages between the inputs of op-amps $AMP_2$ and $AMP_3$. As the closed-loop gain for noise voltages across the resistors $R_A$ and $R_B$ is much smaller than $A_{DIF}$, thermal noise generated by these resistors, as well as current noise generated by the input bias currents of op-amps $AMP_2$ and $AMP_3$, generally does not add significantly to the total amplifier noise.

The design is easily expanded to more channels, as shown in Fig. 3. Each channel amplifies the signal between its input ($E_1 \ldots E_N$) and the $E_0$ reference input (monopolar configuration). Note that the common mode input impedance is equal for all inputs, an important condition to prevent interference (METTINGVANRIJN *et al.*, 1990).

A reduction in the bandwidth can be accomplished with a capacitor parallel to resistor $R_6$. However, appropriate modification of $Z_1$ will then be necessary to retain a high CMRR. A better method is to reduce the gain-bandwidth-product (GBP) of op-amp $AMP_1$ as the CMRR does not depend on the bandwidth of this op-amp. Depending on the type of op-amp, several methods are available; for example, capacitance feedback from the output to one of the offset pins, selection of a proper compensation capacitor (uncompensated op-amps), or the selection of a proper set current (programmable op-amps).

An increased bandwidth can be achieved when an uncompensated op-amp is employed for $AMP_1$. As the ratio of the open-loop gain to the closed-loop gain is small in designs with a high differential gain, stable operation can be realised with much less compensation than is provided in a compensated op-amp (HOROWITZ and HILL, 1989). The application of an uncompensated op-amp is attractive because the power consumption of such an amplifier at a given combination of gain and bandwidth is lower than is the case with the application of a compensated op-amp with a high GBP (see the Appendix).

Latch-up may occur if the common mode input range of op-amps $AMP_2$ and $AMP_3$ is smaller than the output voltage swing of the op-amps $AMP_0$ and $AMP_1$. Therefore, some combinations of op-amps require appropriate output clamping of op-amps $AMP_0$ and $AMP_1$.

The output $AMP_0$ may be used to drive guarding and DRL circuits (METTINGVANRIJN *et al.*, 1990), as shown in Fig. 3. Adding these circuits will effectively reduce the susceptibility to power-line induced interference; the effective CMRR may be increased up to 50 dB at 50 Hz, and interference currents in the electrode leads are prevented.

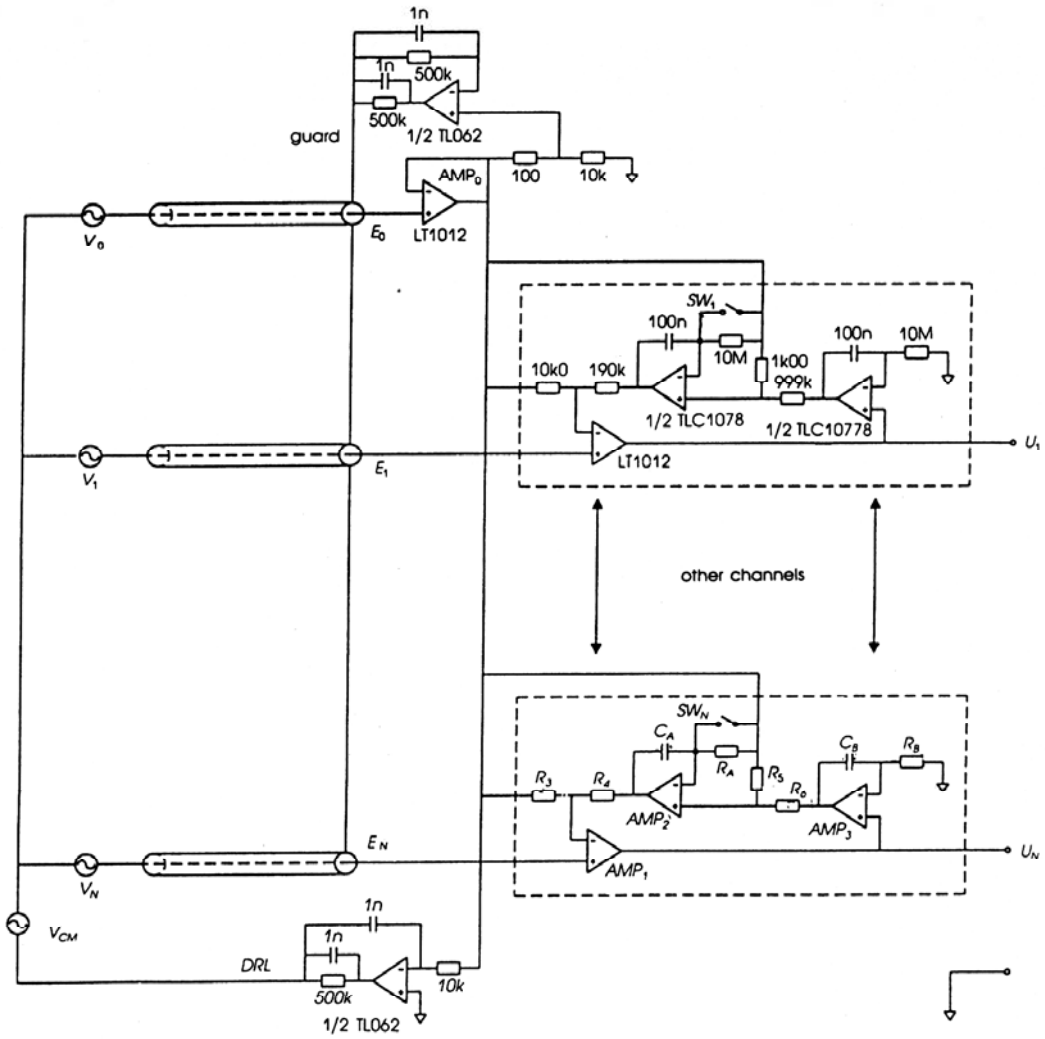


**Fig. 3** *Example of a multichannel EEG amplifier with minimal noise, a low parts count and low power consumption; an extra integrator has been added in the feedback loop to reduce the output offset; a DRL and a guard circuit are used for maximal interference reduction*

In applications with a low differential gain $A_{DIF}$, the closed-loop response of op-amp $AMP_0$ has a relatively large influence on the CMRR. If $Z_1$ is a resistor, the decreasing open-loop gain of $AMP_0$ at higher frequencies results in an increasing closed-loop gain error that, in turn, will lead to a decreasing CMRR at high frequencies. In part, this effect can be counteracted by the use of a capacitor and resistor in parallel for the impedance $Z_1$ ($Z_1 = R_1//C_1$). It can be shown that a good approximation for the optimal value of this capacitor $C_1$ is given by

$$C_1 = \frac{A_{DIF}}{R_1 2\pi GBP_0} \tag{8}$$

where $GBP_0$ is the gain bandwidth product of op-amp $AMP_0$, and $A_{DIF}$ is the differential gain of the amplifier.

On the other hand, in applications with a high differential gain $A_{DIF}$, the CMRR is not significantly degraded if $Z_1$ is omitted and $R_2$ is replaced by a short (see Fig. 3).

The selection of specific components for various applications and the optimisation of the amplifier with respect to various specifications are discussed in detail in the Appendix.

## 5 Discussion

Table 1 gives an impression of the reduction in the number of parts able to be achieved with the design in Fig. 2. In this Table, the circuit in Fig. 2 is compared with a three op-amp design (NEUMAN, 1978) and with a long-tailed pair design (METTINGVANRIJN *et al.*, 1991*a*). All three designs were dimensioned so as to offer a first-order bandpass responses between 0·16 and 100 Hz with a passband gain of 1000. All designs are one-channel differential amplifiers. The circuits are compared without DRL and guard circuits. It follows from Table 1 and the three-op-amp design and the long-tailed pair design require 60% and 100%, respectively, more parts than the design in Fig. 2. It is clear that with the modern trend to record more and more channels (the use of 32 channels is fairly common in clinical EEG, and in experimental settings 64-channel ECG and 128-channel EEG recordings are performed), the savings in cost, dimensions and complexity can be considerable.

The design in Fig. 2 is easily modified for other recordings where small differential AC signals are to be measured in the presence of relatively large differential DC signals and high CM signals. The only restriction is that the overall gain chosen must be relatively high, e.g. more than 1000 with typical component tolerances, or the CMRR is degraded (see eqn. 3).

*Table 1 Number of parts needed for three different designs of amplifiers for bioelectric events*

| | modified two op-amp | three op-amp | long-tailed pair |
|---|---|---|---|
| transistor pairs | 0 | 0 | 2 |
| op-amps | 3 | 4 | 3 |
| resistors | 1 | 10 | 13 |
| capacitors | 1 | 2 | 2 |
| total number of parts | 10 | 16 | 20 |

## 6 Conclusions

A new design is presented that greatly simplifies the design of amplifiers for bioelectric events. The design is easily adapted to various biomedical measurement conditions; i.e. gain, bandwidth and number of channels are easily changed. The specifications are comparable with or better than those achievable with the best designs currently available if proper co-amps are chosen (see the Appendix and Table 1). The design offers major reductions in size and power consumption compared with conventional designs.

*Acknowledgments*—This research was supported by the Technology Foundation (STW).

## References


COOPER, R., OSSELTON, J. W., and SHAW, J. C. (1969): 'EEG technology' (Butterworth, London) pp. 14–22

GEDDES, L. A. (1972): 'Electrodes and the measurements of bioelectronic events' (John Wiley & Sons, New York) pp. 44–94

GRAEME, J. G. (1973): 'Applications of operational amplifiers: third generation techniques' (McGraw-Hill, New York) pp. 53–58

GRAEME, J. G. (1977): 'Designing, with operational amplifiers: application alternatives' (McGraw-Hill, New York) pp. 31–35

HOROWITZ, P., and HILL, W. (1989): 'The art of electronics' (Cambridge University Press, Cambridge) 2nd edn pp. 242–248, pp. 425–428

HUHTA, J. C. and WEBSTER, J. G. (1973): '60-Hz interference in electro-cardiography,' *IEEE Trans.*, **BME-20**, pp. 91–101

METTINGVANRIJN, A. C., PEPER, A., and GRIMBERGEN, C. A. (1990): 'High quality recording of bioelectric events. Part 1: Interference reduction, theory and practice,' *Med. Biol. Eng. Comput.*, **28**, pp. 389–397

METTINGVANRIJN, A. C., PEPER, A., and GRIMBERGEN, C. A. (1991*a*): 'High quality recording of bioelectric events. Part 2: Low-noise, low-power multichannel amplifier design,' *ibid.*, **29**, pp. 433–440

METTINGVANRIJN, A. C., PEPER, A., GRIMBERGEN, C. A. (1991*b*): 'The isolation mode rejection ratio in bioelectric amplifiers,' *IEEE Trans.*, **BME-38**, pp. 1154–1157

NELSON, C. T. (1980): 'Supermatched bipolar transistors improve DC and AC designs,' *Electron. Des. News*, 5 January, pp. 115–120

NEUMAN, M. R. (1978): 'Biopotential amplifiers,' *in* WEBSTER, J. G. (Ed.): 'Medical instrumentation: application and design.' (Houghton Mifflin Co., Boston) pp. 307–309

PACELA, A. F. (1967): 'Collecting the body's signals,' *Electronics*, **40**, (14), pp. 103–112

SILVERMAN, D., MASLAND, R. L., SAUNDERS, M. G., and SCHWAB, R. S. (1969): 'Minimal electroencephalographic recording techniques in suspected cerebral death,' *Electroenceph. Clin. Neurophysiol.*, **29**, pp. 731–732

SMIT, H. W., VERTON, K., and GRIMBERGEN, C. A. (1987): 'A low-cost multichannel preamplifier for physiological signals, *IEEE Trans.*, **BME-34**, pp. 307–310

TOBEY, G. E., GRAEME, J. G., and HUELSMAN, L. P. (1971): 'Operational amplifiers: design and applications' (McGraw-Hill, New York) pp. 205–207


## Appendix

### *Multichannel EEG amplifier*

An example of the component selection for a low-noise multichannel EEG amplifier with a minimal number of parts is given in Fig. 3. $AMP_0$ and $AMP_1$ are bipolar low-power op-amps with low voltage and current noise and good output drive capabilities (LT1012 single op-amp). The GBP of these op-amps (800 kHz) is sufficiently high to provide a differential gain of 20 000 in a passband of 0·16–40 Hz. $AMP_2$ and $AMP_3$ are linear CMOS micropower precision op-amps (TLC1078 dual op-amp), with a low input offset voltage (0·2 mV typical) and an extremely low input bias current (0·6 pA typical).

The op-amps used in the DRL and guarding circuits (TL062 dual op-amp) were selcted for low power consumption, high GBP and proper compensation for unity gain operation. The DC output current of the DRL and guard circuits has been limited to 10 $\mu$A in order to protect the patient from amplifier faults.

The key specifications of the amplifier are listed in Table 2. Each channel is equipped with a 'deblock' switch ($SW_1 \ldots SW_N$ in Fig. 3) for quick recovery after overload conditions. Operation of the switch can either be manual or automatic using an additional overload detection circuit.

The bandwidth and/or gain may be increased by using an uncompensated op-amp for $AMP_1$. For example, with LT1008, which is an uncompensated version of the LT1012, the bandwidth can be increased by a factor of 50 at the same power consumption. External compensation is not necessary for stable operation in this case (the LT1008 is stable for a closed-loop gain $>200$). However, an external compensation capacitor may be used to tune the bandwidth for a specific application. All specifications given in Table 2, except the noise figures, are still valid when an LT1008 is used for $AMP_1$. Of course, the total input noise increases proportionally to the square root of the bandwidth of the amplifier.

The design described above was optimised for EEG measurements, where high differential gain and low noise are of prime importance. The design may be optimised with respect to other parameters. For example, if minimal power consumption is pursued, the use of a modern micropower op-amp for $AMP_1$ would offer a large reduction in power consumption, and application of the LT1077 would reduce the power consumption for $N$ channels to (8 + $N$*0·8) mW (at $\pm$5 V supply voltage).

However, as these op-amps offer a lower GBP (200 kHz), the differential gain and/or the bandwidth of the amplifier have to be reduced. In addition, the output stage of the LT1077 is inferior to that of the LT1012 in terms of output impedance and maximum output current. The total equivalent input noise is approximately 20% higher.

A lower noise with the source impedances encountered in EEG recordings (the electrodes, 3–30 k$\Omega$) is not attainable with current commercially available op-amps. There are several op-amps available that offer a lower voltage noise, for example, LT1001, LT1007 and LT1028. However, the current noise of these op-amps is higher by a factor of 10–1000 than that of the LT1012. As electrode impedances lower than several k$\Omega$ cannot be reliably reproduced in typical EEG recordings, application of these op-amps would usually increase the total equivalent input noise. In ECG recordings, the electrode impedances are usually higher by a factor of 10 owing to less extensive skin preparation, making a low current noise even more important.

In recordings with depth electrodes (impedance $>1$ M$\Omega$), a low current noise is of prime importance, and, in this case, a low-noise op-amp with FET inputs, such as LT1055, OPA111 or TLC2201, would be a good choice. The power consumption of these

*Table 2 Specifications of the amplifier for bioelectric events shown in Fig. 3**

| | |
|---|---|
| equivalent input noise voltage, $\mu V_{rms}$, 0·2–40 Hz | = 0·15 |
| equivalent input noise current, $pA_{rms}$, 0·2–40 Hz | = 1 |
| bandwidth (+0/−3 dB), Hz | = 0·2–40 |
| passband gain | = 20 000 |
| differential AC input range, $mV_{pk-Pk}$ | = 0·4 |
| differential DC input range, $mV_{pk-pk}$ | = 200 |
| common mode rejection ratio†, dB at 50 Hz | = 136 |
| common mode input range, V | = +4−−4 |
| output offset, mV | = <1 |
| total distortion§ | = <0·1% |
| power consumption for $N$ channels, mW | = {8 + $N$*4} |

* all specifications are at a supply voltage of $\pm$5 V.
† a DRL circuit was used to decrease the common mode voltage with 50 dB at 50 Hz.
§ measured with an input signal of 10 Hz, 100 $\mu V_{pk-pk}$; the magnitudes of the distortion products were below the noise level of the amplifier.

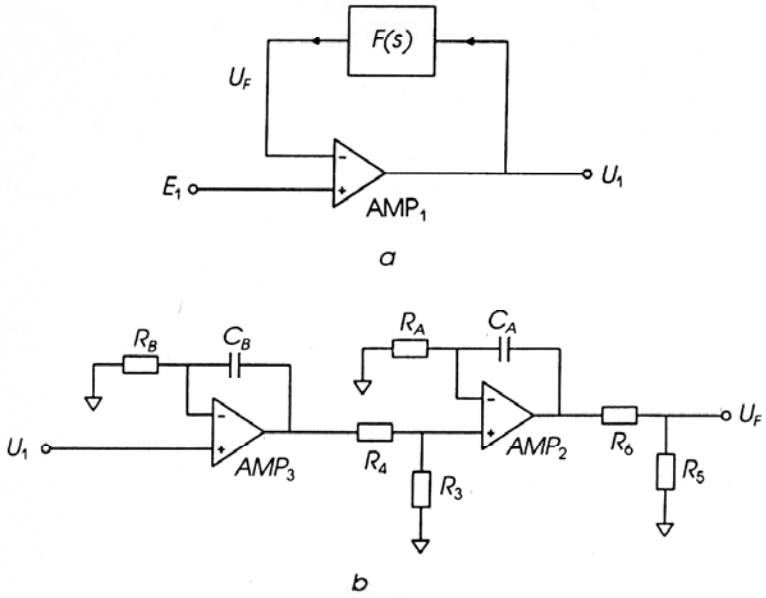


**Fig. 4** *(a) Equivalent circuit representing the amplifier designs shown in Figs. 2 and 3, with the input $E_0$ connected to common (0 V); transfer function $H(s)$ of the equivalent amplifier circuit is given in eqn. 10; (b) Schematic of the feedback circuit of the equivalent amplifier circuit in (a); transfer function $F(s)$ of the feedback circuit is given in eqn. 9*

op-amps, however, is higher by a factor of 5–10 than that of the LT1012.

*Stability*

The stability of the design is evaluated with input $E_0$ connected to common (0 V). The designs of Figs. 2 and 3 can then be replaced by the circuit in Fig. 4*a*, where $H(s)$ is the transfer function of the complete circuit and $F(s)$ is the transfer function of the feedback circuit (Fig. 4*b*). Here the more complicated feedback circuit with two integrators, shown in Fig. 3, is described. The results are readily applied to the feedback circuit with a single integrator shown in Fig. 2. The circuit in Fig. 2 can be regarded as a special case of the circuit in Fig. 3.

Here all op-amps are assumed to be of the internally compensated type.

The transfer function of the feedback circuit (Fig. 4*b*), which consists of two potential dividers ($R_3$, $R_4$ and $R_5$, $R_6$) and two integrators ($AMP_2$ and $AMP_3$), is given by

$$F(s) = \frac{U_F}{U_1} = \frac{A_2A_3(1 + s\tau_B)(1 + s\tau_C)}{A_{DIF}[(1 + s\tau_2)(1 + s\tau_B) + A_2s\tau_B][(1 + s\tau_3)(1 + s\tau_C) + A_3s\tau_C]} \quad (9)$$

where $A_2$, $A_3$ are the DC open-loop voltage gains of op-amps $AMP_2$ and $AMP_3$; $\tau_2$, $\tau_3$ are time constants of the first poles of op-amps $AMP_2$ and $AMP_3$; $\tau_A = R_AC_A$ (a high-pass time constant); $R_B = R_B C_B$ (a high-pass time constant); and $A_{DIF}$ is the differential passband-gain given in eqn. 5.

The transfer function $H(s)$ of the total amplifier circuit is given by

$$H(s) = \frac{U_1}{E_1} = \frac{A_1}{1 + s\tau_1 + A_1F(s)} \quad (10)$$

where $A_1$ is the DC open-loop voltage gain of $AMP_1$; $\tau_1$ is the time constant of the first pole of $AMP_1$; and $F(s)$ is the transfer function of the feedback circuit.

The transfer function $H(s)$ has five poles and four zeros. However, with the time constant and voltage gains typical in measurements of bioelectric events, one pole-pair almost coincides with one zero-pair, whereas the other poles and zeros are situated very close to the real axis. Consequently, $H(s)$ can be approximated very well by a transfer function with three real poles and two real zeros:

$$H_{approx}(s) = \frac{A_{DIF}(1 + s\tau_BA_2)(1 + s\tau_0A_3)}{A_2A_3(1 + s\tau_B)(1 + s\tau_C)[1 + s\tau_1(A_{DIF}/A_1)]} \quad (11)$$

where $A_1$, $A_2$, $A_3$ are DC open-loop voltage gains of op-amps $AMP_1$, $AMP_2$ and $AMP_3$; $\tau_1$ is the time constant of the first pole of op-amps $AMP_1$; $\tau_A = R_AC_A$ (a high-pass time constant); $\tau_B = R_BC_B$ (a high-pass time constant); $A_{DIF}$ is the differential passband-gain given in eqn. 5.

For example, if a gain $A_{DIF}$ of 10 000 is chosen in the passband between 0·16 and 30 Hz and typical op-amp parameters are assumed ($A_1$, $A_2$, and $A_3$ = 300 000, and $\tau_1$, $\tau_2$ and $\tau_3$ = 0·16), it can be shown that the maximal amplitude difference between the transfer functions $H(s)$ and $H_{approx}(s)$ is 0·2 dB, and the maximal phase difference is 0·9°.

As differences between $H(s)$ and $H_{approx}(s)$ are insignificant for typical biomedical implementations, the behaviour of the amplifiers in Figs. 2 and 3 can be evaluated with the approximating transfer function $H_{approx}(s)$. The circuit described by the transfer function $H_{approx}(s)$ is stable because the poles are situated in the left half of the complex $s$-plane, and there are no resonances because the poles are on the real $s$-axis.

## Author's biography

Alexander C. MettingVanRijn (aged 33) received his degree in Physics in 1987 at the Unversity of Amsterdam. Since then he has been working in the Laboratory of Medical Physics & Informatics at the university on a five-year project sponsored by the Technology Foundation (STW) for the development of telemetry systems for biomedical recordings. During this time, project amplifiers and optical transmission systems (with optical fibre and wireless) have been developed that are described in several published papers. This paper is part of the PhD thesis he is currently preparing.